Quasi phase matching in GaAs–AlAs superlattice waveguides through bandgap tuning by use of quantum-well intermixing

A. Saher Helmy, D. C. Hutchings, T. C. Kleckner, J. H. Marsh, A. C. Bryce, J. M. Arnold, C. R. Stanley, and J. S. Aitchison

Department of Electronics and Electrical Engineering, University of Glasgow, Glasgow G12 8QQ, UK

C. T. A. Brown, K. Moutzouris, and M. Ebrahimzadeh

School of Physics and Astronomy, University of St. Andrews, St. Andrews, Fife KY16 9SS, UK

Received April 6, 2000

We report the observation of second-harmonic generation by type I quasi phase matching in a GaAs–AlAs superlattice waveguide. Quasi phase matching was achieved through modulation of the nonlinear coefficient $\chi^{(2)}_{zxy}$, which we realized by periodically tuning the superlattice bandgap. Second-harmonic generation was demonstrated for fundamental wavelengths from 1480 to 1520 nm, from the third-order gratings with periods from 10.5 to 12.4 μm. The second-harmonic signal spectra demonstrated narrowing owing to the finite bandwidth of the quasi-phase-matching grating. An average power of ~110 nW was obtained for the second harmonic by use of an average launched pump power of ≤2.3 mW. © 2000 Optical Society of America

OCIS codes: 190.5970, 190.2620, 160.4330.

The use of second-order nonlinearities in III–V semiconductors, which have intrinsically large $\chi^{(2)}$ coefficients, offers the possibility of efficient optical frequency conversion. The mature GaAs-based fabrication technology and the potential for direct integration with laser diodes could lead to the development of numerous functional devices,[1,2] ranging from second-harmonic-generation structures to integrated devices for difference frequency generation (with applications in wavelength-division multiplexed channel conversion[3]), parametric amplification, and oscillation. Because of the lack of intrinsic birefringence in III–V semiconductor structures and the large normal dispersion, it is difficult to phase match the second-order nonlinear process. Recently a technique was developed to induce an artificial birefringence by means of embedding native oxide layers in the waveguide, but work is still in progress to overcome the excessive optical losses incurred in these waveguides.[4] Greater flexibility is possible with quasi phase matching (QPM), and in initial studies of semiconductors, domain inversion by use of growth on patterned substrates was investigated.[5,6] Although promising, patterned substrate growth is still associated with high optical losses and low yield.

An alternative technology, described here, is domain-disordering QPM obtained by postgrowth sample processing. Modulation of $\chi^{(2)}$ in semiconductor waveguides was previously obtained by amorphization with implantation.[7] Here we realize domain-disordering QPM through the modulation of the heterostructure bandgap while preserving the crystalline structure, which subsequently provides modulation in the bulklike $\chi^{(2)}_{xyz}$ and $\chi^{(2)}_{zxy}$ coefficients when operating near a material resonance. The values of this modulation in GaAs–AlAs superlattices are predicted to be as large as those attained in periodically poled $LiNbO_3$.[8] The bandgap modulation is achieved by use of quantum-well intermixing (QWI), by which lateral control over the heterostructure bandgap can be obtained with no substantial increase in optical losses.[9] In addition, domain-disordering QPM by use of QWI is attractive because it is based on nondestructive, postgrowth, lithography-based semiconductor fabrication. One can also use QWI with asymmetric heterostructures to modulate additional induced $\chi^{(2)}$ tensor elements,[10] but these coefficients tend to be relatively small (typically a few pm V^{-1}).[11]

In this Letter we present measurements of second-harmonic generation from third-order quasi-phase-matched gratings achieved with QWI. The structure used was composed of 0.6 μm of a symmetric superlattice waveguide core made of 14:14 monolayers of GaAs:AlAs. The lower and upper claddings were bulk $Al_{0.6}Ga_{0.4}As$ of 4 and 1.5 μm width, respectively. A 100-nm GaAs cap was used to cover the upper cladding. The structure was nominally undoped and grown by molecular beam epitaxy on a semi-insulating GaAs substrate. The room-temperature photoluminescence emission wavelength of the structure was 745 nm from the central portion of the wafer. This design will allow an operating fundamental wavelength of ~1550 nm at 30 meV below the half-bandgap, allowing us to avoid two-photon absorption and use the modulation attained in the resonant component of $\chi^{(2)}$ as the bandgap of the structure is shifted. We achieved domain disordering by use of sputtered silica defect–induced intermixing[12] with electron-gun-deposited silica caps to suppress the process. The sputtered-silica intermixing process does not introduce any significant optical loss; for example, the band-edge absorption is reduced to just 4 cm^{-1} in a InGaAs–InGaAsP laser structure.[13] After annealing of the present sample, the room-temperature photoluminescence peaks were observed at 725 and 680 nm; the peaks originated from the suppressed and the disordered regions, respectively.

The optical source used in the measurements is a synchronously pumped singly resonant femtosecond periodically poled $LiNbO_3$ optical parametric oscillator (OPO) based on a semimonolithic cavity design. The OPO was pumped by a Kerr-lens mode-locked

0146-9592/00/181370-03$15.00/0

Ti:sapphire laser at 820 nm that provided pulses of ~100-fs duration at an 80-MHz repetition rate. An average power of 80 mW was obtained from the OPO before chopping with a 50% duty cycle for lock-in detection. A 4-mm-long sample with grating periods from 5.8 to 12.4 μm was mounted on an end-fire coupling rig. TE-polarized light from the OPO was launched into the waveguide, and the output of the waveguides was aligned into a monochromator. A photomultiplier tube (PMT) was then used to detect the second harmonic at the output of the monochromator with an internal PMT amplifier and a lock-in amplifier. The PMT has a spectral range 185–900 nm, and therefore no signal from the fundamental could be detected. We plotted the power into the waveguide as a function of the detected fundamental power at the waveguide output to ensure a linear relation, confirming that there was no significant two-photon absorption of the fundamental.

The periodic modulation in the superlattice bandgap induces a modulation in $\chi^{(2)}$, as illustrated in Fig. 1, in which intermixing occurs under the sputtered silica caps only. There are two possible phase-matching geometries: (1) type I phase matching exploits the modulation in $\chi^{(2)}_{zxy}$, which we obtain by launching the fundamental TE polarized at the input and the second-harmonic that is expected with TM polarization, and (2) type II phase matching that exploits the modulation in $\chi^{(2)}_{xyz}$, accessible with mixed TE:TM polarization for the fundamental and the second harmonic is expected with TE polarization. These two cases will be phase matched at different QPM grating periods as a result of the variation in propagation constant with polarization mode. The superlattice breaks the degeneracy between $\chi^{(2)}_{xyz}$ and $\chi^{(2)}_{zxy}$ that exists in bulk semiconductors with a zinc-blende structure but is restored on QWI, with the larger modulation predicted for $\chi^{(2)}_{xyz}$.[8]

A typical measurement of the type I SH spectra is shown in Fig. 2, in which there is a clear second-harmonic signal for TM polarization and no signal for the TE. The measured bandwidth of the second-harmonic (FWHM, 3 nm) is limited by the finite width of the monochromator slit at an acceptable signal-to-noise ratio, whereas the measured FWHM is 11 nm for the fundamental. Therefore additional spectral narrowing occurs, owing to the fact that the bandwidth of the QPM grating is smaller than that of the input optical pulse. The second-harmonic signal appears only when the output spectrum of the OPO is tuned so that it contains the appropriate wavelength for the QPM grating under test. Figure 3 shows a typical result for the dependence of the second-harmonic power on the fundamental power. The best fit to the slope on a log–log plot is 1.9, confirming the expected parabolic power dependence with no observed saturation. The wavelength of the SH generated as a function of various grating periods available in the sample is plotted in Fig. 4. As the grating period is decreased the QPM wavelength also decreases in this normally dispersive medium. The lower wavelength limit is reached when the second-harmonic photon energy approaches the material bandgap and experiences excessive band-edge absorption.

At the PMT the largest average second-harmonic power measured was 25 nW for a wavelength of 758 nm. However, the optical measurement system has a measured 5-dB loss between the waveguide and the PMT, and with a further 30% reflection loss at the rear facet of the waveguide we can specify the best average second-harmonic power of ~110 nW in the

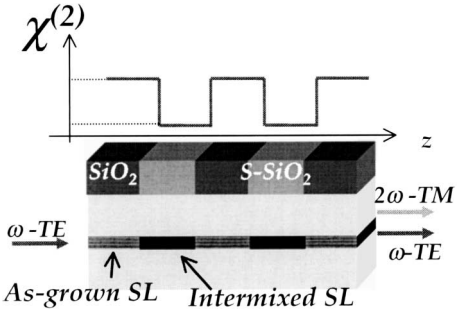

Fig. 1. Illustration of the type I second-harmonic generation process, in which we modulate the resonant part of the $\chi^{(2)}_{zxy}$ bulk coefficient by selective area QWI to achieve QPM. SL's, superlattices.

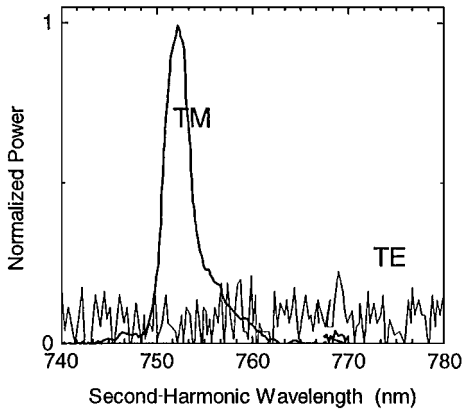

Fig. 2. Typical second-harmonic spectra showing both output polarizations. The waveguide used in this example has a QPM grating period of 12.4 μm.

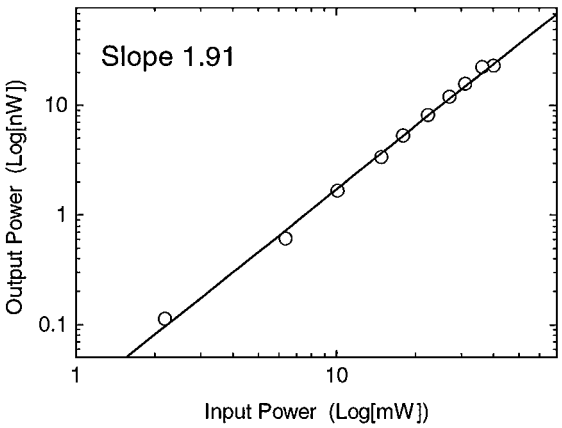

Fig. 3. Second-harmonic output average power (measured at the PMT) as a function of the fundamental input average power (measured after the chopper) on a log–log scale. The best fit to the slope is 1.9, confirming the expected parabolic power dependence.

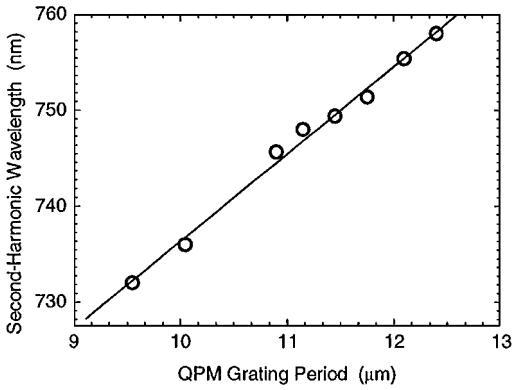

Fig. 4. Tuning curve indicating the second-harmonic wavelength as a function of the QPM grating period in the waveguides.

waveguide. In this case we measure a transmitted fundamental average power of 250 μW, which, with a 30% loss at the rear facet and measured optical loss of $\sim$2 dB/nm in the waveguide, translates to an average pump power of $\lesssim$2.3 mW just after the front facet of the waveguide. We note that there is a reduction of approximately 2 orders of magnitude in fundamental power between the OPO output and the guided mode, which is due principally to coupling losses.

Hence we obtain a maximum second-harmonic conversion of $\sim$0.02% with the present setup, for which there is considerable room for improvement: (1) The coupling losses at present severely limit the fundamental power launched into a guided mode by the end-fire rig. (2) The femtosecond optical source has a bandwidth larger than the QPM grating, and hence the majority of the guided fundamental power is not phase matched. Furthermore, dispersion will result in significant temporal broadening of the fundamental pulse as it propagates in the waveguide. A transform-limited picosecond source would avoid both of these restrictions. (3) In this sample we have used a third-order grating because of initial concerns about the resolution of the intermixing process. However, the period of the grating for phase matching is larger than our first estimates, and first-order gratings should be acceptable, with potentially an order-of-magnitude improvement in conversion efficiency. Indeed, we were able to observe second-harmonic generation by first-order QPM, using our shortest grating period at the long-wavelength limit of our optical source. (4) Preliminary spatially resolved photoluminescence studies indicate that there may be some residual intermixing under the electron-gun-deposited silica caps plus a degree of lateral spreading. Hence the depth of modulation of the nonlinearity has room for improvement by reduction of the upper cladding layer and further optimization of the sample processing.

In conclusion, second-harmonic generation by type I quasi phase matching in GaAs–AlAs superlattice waveguides has been demonstrated. QPM was achieved through modulation of the bulklike nonlinear coefficient $\chi^{(2)}_{zxy}$, which was realized by periodic tuning of the superlattice bandgap with quantum-well intermixing. Although there will be an associated modulation of the refractive index, this is minimal in the vicinity of the half-bandgap, and hence the observed efficiency of the process in a third-order grating is far larger than can be attributed soley to a refractive-index change.[14] Second-harmonic generation was demonstrated for fundamental wavelengths from 1480 to 1520 nm, from third-order gratings with periods from 10.5 to 12.4 μm. The second-harmonic signal spectra were found to exhibit spectral narrowing owing to the finite QPM bandwidth. An average power of $\sim$110 nW was obtained for the second harmonic with an average pump power of $\lesssim$2.3 mW.

The authors thank M. W. Street and D. Ortega of the University of Glasgow and P. Martin and J. P. Landesman of Thomson–CSF for valuable assistance. D. C. Hutchings thanks the Engineering and Physical Sciences Research Council for its support through an Advanced Fellowship. M. Ebrahimzadeh thanks the Royal Society of London for its support through a University Research Fellowship. This work was carried out under the European Union European Strategic Programme for R&D in Information Technology project OFCORSE II.

References

1. J. S. Aitchison, M. W. Street, N. D. Whitbread, D. C. Hutchings, J. H. Marsh, G. T. Kennedy, and W. Sibbett, IEEE J. Sel. Top. Quantum Electron. **4,** 695 (1998).
2. J. B. Khurgin, E. Rosencher, and Y. J. Ding, J. Opt. Soc. Am. B **15,** 1726 (1998).
3. S. J. B. Yoo, J. Lightwave Technol. **14,** 955 (1996).
4. A. Fiore, S. Janz, L. Delobel, P. van der Meer, P. Bravetti, V. Berger, and E. Rosencher, Appl. Phys. Lett. **72,** 2942 (1998).
5. S. J. B. Yoo, R. Bhat, C. Caneau, and M. A. Koza, Appl. Phys. Lett. **66,** 3410 (1995).
6. C. B. Ebert, L. A. Eyres, M. M. Fejer, and J. S. Harris, Jr., J. Cryst. Growth **202,** 187 (1999).
7. S. Janz, M. Buchanan, F. Chatenoud, J. P. McCaffrey, R. Normandin, U. G. Akano, and I. V. Mitchell, Appl. Phys. Lett. **65,** 216 (1994).
8. D. C. Hutchings, Appl. Phys. Lett. **76,** 1362 (2000).
9. C. J. Hamilton, J. H. Marsh, D. C. Hutchings, J. S. Aitchison, G. T. Kennedy, and W. Sibbett, Appl. Phys. Lett. **68,** 3078 (1996).
10. M. W. Street, N. D. Whitbread, C. J. Hamilton, B. Vögele, C. R. Stanley, D. C. Hutchings, J. H. Marsh, J. S. Aitchison, G. T. Kennedy, and W. Sibbett, Appl. Phys. Lett. **70,** 2804 (1997).
11. D. C. Hutchings and J. M. Arnold, Phys. Rev. B **56,** 4056 (1997).
12. O. P. Kowalski, C. J. Hamilton, S. D. McDougall, J. H. Marsh, A. C. Bryce, R. M. De La Rue, B. Vögele, C. R. Stanley, C. C. Button, and J. S. Roberts, Appl. Phys. Lett. **72,** 581 (1997).
13. S. D. McDougall, O. P. Kowalski, C. J. Hamilton, F. Camacho, B. Qiu, M. Ke, R. M. De La Rue, A. C. Bryce, and J. H. Marsh, IEEE J. Sel. Top. Quantum Electron. **4,** 636 (1998).
14. M. M. Fejer, G. A. Magel, D. H. Jundt, and R. L. Byer, IEEE J. Quantum Electron. **28,** 2631 (1992).